Journal of Materials Processing Technology 229 (2016) 668–677

Contents lists available at ScienceDirect

Journal of Materials Processing Technology

journal homepage: www.elsevier.com/locate/jmatprotec

Effect of metal micro-structuring on the mechanical behavior of polymer–metal laser T-joints

E. Rodríguez-Vidal[a,*], C. Sanz[a], C. Soriano[a], J. Leunda[a], G. Verhaeghe[b]

[a] IK4-TEKNIKER, Polo Tecnológico de Eibar, Calle Iñaki Goenaga 5, 20600 Eibar, Gipuzkoa, Spain
[b] Faurecia Autositze GmbH, Nordsehler Strasse 38, Stadthagen 31655, Germany

ARTICLE INFO

Article history:
Received 3 August 2015
Received in revised form 20 October 2015
Accepted 22 October 2015
Available online 28 October 2015

Keywords:
Polymer–metal hybrid joints
Laser joining
Laser structuring
Glass fiber reinforced polymers
T-joints

ABSTRACT

The metal was locally structured by pulsed laser radiation producing microscopic patterns on its surface. In a second step the opposite side of the micro-structured metal was irradiated by a continuous wave (CW) fiber laser to achieve the mechanical interlock between the two materials. A tight relationship between the microstructure parameters and pull-out test performance was observed. The greatest strength was achieved when the distance between subsequent grooves was minimized. The T-joint mechanical performance did not reveal any significant dependence on the considered range of joining areas. The morphological and topographical features of the detached surfaces showed that the micro-structured grooves were completely filled during the laser conductive joining process. Different alignment angles of patterns produced different failure modes although there was no evidence of an additional mechanical interlock.

1. Introduction

Direct thermal laser joining of plastic and metallic materials is nowadays arising as an alternative technology for the generation of sound hybrid joints. Depending on the optical properties of the polymer at the source wavelength, two variants exist. In laser transmission joining, the polymer is highly transparent to the laser radiation and the laser beam reaches the interface without being absorbed by the polymer. By contrast, in conduction joining, the polymer is opaque to the laser wavelength, so the metal surface opposite to the interface is directly irradiated by the laser beam, and the heat is transported by conduction to the interface, thus heating up the polymer.

The laser joining approach was first demonstrated at the Joining and Welding Research Institute of Osaka University by Kawahito et al. (2006) and Katayama et al. (2007). In these pioneering studies, joints between stainless steel and polyethylene terephthalate (PET), polyamide (PA), polycarbonate (PC) and polypropylene (PP) were generated. High shear strength was achieved, suggesting the presence of both chemical and physical bonding. Since then, the technique has been extended to various material combinations, such as DC01 steel to PA6.6, Bergmann and Stambke (2012), aluminum to PC, PA and glass fiber reinforced polyamide, Amend et al. (2013), 304 stainless steel to PMMA, Hussein et al. (2013) and zinc-coated steel to carbon fiber reinforced polyamide, Jung et al. (2013).

Nowadays, metal-polymer assemblies are replacing fully metallic parts in several applications for the automotive sector, as well as in non-automotive applications ranging from appliance housings to bicycle frames (Cenigaonaindia et al. (2012)). However, the direct laser joining of hybrid assemblies is still in a development stage for industrial use and a deeper research has to be carried out. The mechanical performance of the produced assemblies has to be improved while the cycle time is reduced. The latter is directly related to the continuous development of high brightness laser sources.

Different approaches for polymer–metal hybrid joining were reviewed by Grujicic et al. (2008), concluding that the one based on micro-scale mechanical interlocking is the most promising method. A way to further enhance the hybrid joint performance is to generate microstructures on the metal surface, so as to produce surface irregularities that provide an extra mechanical interlock with the melted polymer. A greater control of the surface geometry on a micrometric scale becomes important for hybrid polymer–metal joints. Laser microprocessing with pulsed sources is probably the most advanced technique developed for microprocessing of mechanical components due to its promising peculiarities.

* Corresponding author.
E-mail address: eva.rodriguez@tekniker.es (E. Rodríguez-Vidal).

http://dx.doi.org/10.1016/j.jmatprotec.2015.10.026

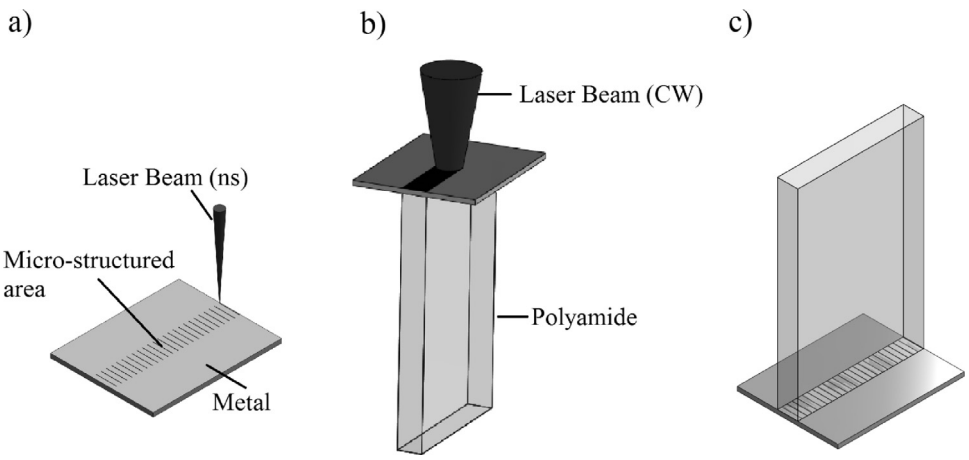

Fig. 1. Scheme of (a) texturing process; (b) joining process; (c) T-joint configuration.

During the last four years, several studies have been reported based on the effect of laser structure parameters on the mechanical properties of hybrid polymer–metal joints. Roesner et al. (2011) reported the effect of structure density (defined as the ratio of the structured area to the overall examined area) generated during the laser metal pre-treatment on the mechanical behavior of hybrid joining (steel–polyamide) conducted by induction technique. Cenigaonaindia et al. (2012) analyzed the feasibility of using the laser technology to develop an adhesive free method for joining PA6-AISI304. They analyzed the effect of three metal surface textures machined on the metal in order to evaluate their influence on the polymer flow. Amend et al. (2013) explored the hybrid joining of aluminum 5182 with three different thermoplastics (PC, PA6 and PA66-GF30). The study showed a pre-treatment of the aluminum surface carried out by nanosecond laser pulses, analyzing the influence of two different surface textures (grid and craters) on tensile shear strength. Schricker et al. (2014) examined the influence of geometrical features of macroscopic structures generated by milling process on load capacity for aluminum 6082-PA66 joints. Amend et al. (2014) explored the direct joining between aluminum and PC, PA6 and PA66-GF30, performed by means of mono- and polychromatic radiation with the pre-treatment process produced by nanosecond pulses. They evidenced a clear dependence of the absorption percentage of aluminum with the microstructure density, being the higher microstructure density the higher absorption values. Heckert and Zaeh (2014) reported the potential of laser processed surface structures in the macroscopic, microscopic and nanoscopic scale as metal pre-treatment which can be used for thermal joining of three different fiber reinforced thermoplastics with aluminum. Rodríguez-Vidal et al. (2014) studied the influence of different microstructure geometries on the joint's tensile-shear mechanical performance of steel–fiber reinforced polyamide assemblies. Both the micro-structuring and the joining operations were conducted by laser sources.

The studies cited above report the influence of the metal pre-treatment on the mechanical performance obtained by tensile shear tests. However no previous study examined the impact of microstructure parameters on the mechanical behavior of T-assemblies with dissimilar materials. The T-configuration becomes significant to explore the mechanical performance of the dissimilar assemblies in the real application.

The focus of the research is on analyzing the influence of the metal pre-treatment on the mechanical performance of T-joints of opaque fiber reinforced polyamide to HC420LA steel. Both the micro-structuring and the joining are conducted by laser sources. The effect of a wide range of microstructure parameters on pull-out strength is discussed.

2. Materials and experimental procedure

Materials used in this work were a low alloy steel (HC420LA) and a glass fiber reinforced polyamide (PA6-GF30). $25 \times 20 \times 0.8$ mm metal plates were joined to polyamide samples with two different thicknesses, $40 \times 25 \times 2.5$ mm and $40 \times 25 \times 4$ mm, in order to analyze whether the joining area affects the results, since a small joining area of these dissimilar materials is a geometrical request of the final assembly.

Metal specimens were laser structured with selected texture patterns by a nanosecond fiber laser source (Fig. 1a). Laser beam movement was produced by a 2D galvo scanning system, capable of scanning structure patterns at high speed. The cross sections of the specimens were mounted into Epoxy resin to analyze the depth, recast material and alignment angle of the engraved structure by optical microscopy. Ten different measurements of groove depth and alignment angle were carried out for each set of microstructure conditions.

Subsequently the opposite side of the microstructured metal was irradiated by a CW fiber laser source, clamping the polymer and metal samples in a T configuration (Fig. 1b). In this operation, the laser beam was also guided and focused on the workpiece by a 2D galvo scanning unit. The laser energy is first absorbed on the metal surface and then transferred by conduction to the surrounding area, generating the melting of the polymer and producing the joint after solidification (Fig. 1c). The joining parameters were kept constant (laser power $P = 74$ W and joining speed $v = 6$ mm/s) in order to study the influence of different microstructure patterns on the mechanical response of the T-joints. Both materials were clamped by applying a uniform pressure (P=3 bar) with a pneumatic clamping device, in order to enhance the flow of the molten plastic material into the microstructures of the steel.

The mechanical properties of the T-joints were analyzed by pull-out tests to measure the joint strength. The latter was represented by the failure force (load at which the joint breaks into two separate pieces) divided by the contact area (2.5×25 mm^2 and 4×25 mm^2 for 2.5 mm and 4 mm polyamide thickness respectively). The T-joints were tested by a INStron 3369 Static Universal machine with a maximum load capacity of 50 kN and a cross-head displacement rate of 5 mm/min (Fig. 2a). T-Joint samples were mounted in the INStron grips using a tailored clamping device (Fig. 2b). For each experimental condition, five specimens were tested to ensure the reproducibility of the results.

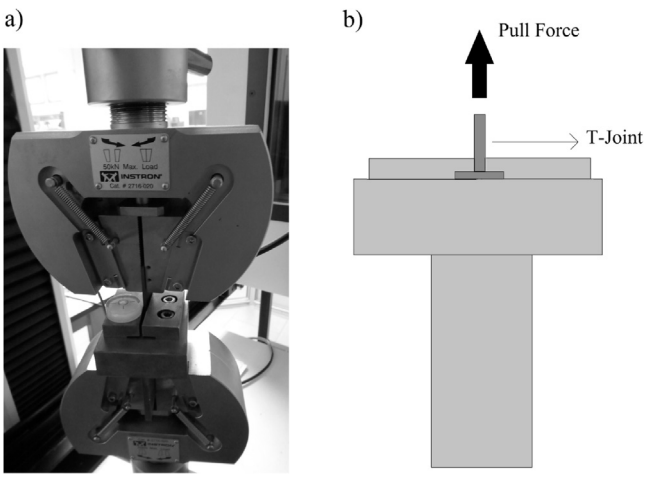

Fig. 2. (a) Experimental set-up for measuring the joint failure force during pull-out tests; (b) schematic view of pull-out test device.

After pull-out tests the fracture surfaces (joining interfaces of both metallic and polymer parts) were characterized in terms of their morphology and topography in order to find out a direct relation between the joint strength values and the amount of melted polymer introduced into the microstructures during the joining process. The morphological and topographical characterizations of the fracture surfaces were carried out by Scanning Electron Microscopy (SEM) (Karl Zeiss XB1540) and mechanical stylus profilometry (Dektak 8, Veeco) respectively. For topographical characterization, 2 mm long profiles were measured on the microstructured metal surface, across the grooves. Three measurements were carried out in each plate to guarantee the homogeneity of the produced microstructure.

3. Laser micro-structuring of steel

The microstructure patterns, consisting of parallel grooves, were defined in terms of the groove depth (d in Fig. 3a), groove width (w in Fig. 3a), the distance between adjacent grooves ($d_{c\text{-}c}$ in Fig. 3a), the alignment angle of the laser beam (θ in Fig. 3b) and the orientation of grooves with respect to the weld track (Fig. 3c). The alignment angle specifies the angle between the propagation direc-

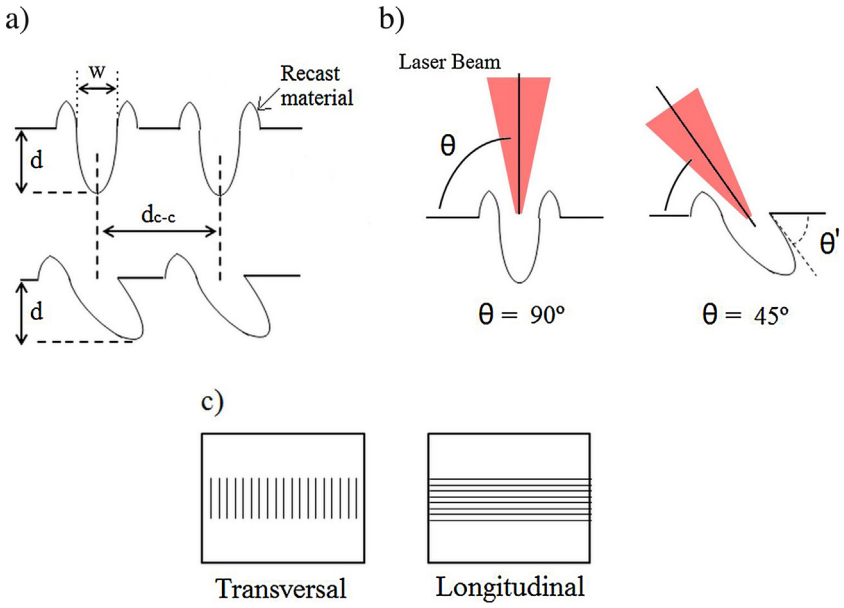

Fig. 3. Schematic laser structure surface and relevant characteristics.

Table 1
Relevant microstructure parameters.

	Factor levels	N_{tracks} 2, 4	$d_{c\text{-}c}$ [μm] 200, 600	Alignment angle θ [°] 90, 45	Orientation Trans, Long
Microstructure Conditions [MC]	1	2	200	90	Trans
	2	2	200	90	Long
	3	4	200	90	Trans
	4	4	200	90	Long
	5	2	600	90	Trans
	6	2	600	90	Long
	7	4	600	90	Trans
	8	4	600	90	Long
	9	2	200	45	Trans
	10	2	200	45	Long
	11	4	200	45	Trans
	12	4	200	45	Long
	13	2	600	45	Trans
	14	2	600	45	Long
	15	4	600	45	Trans
	16	4	600	45	Long

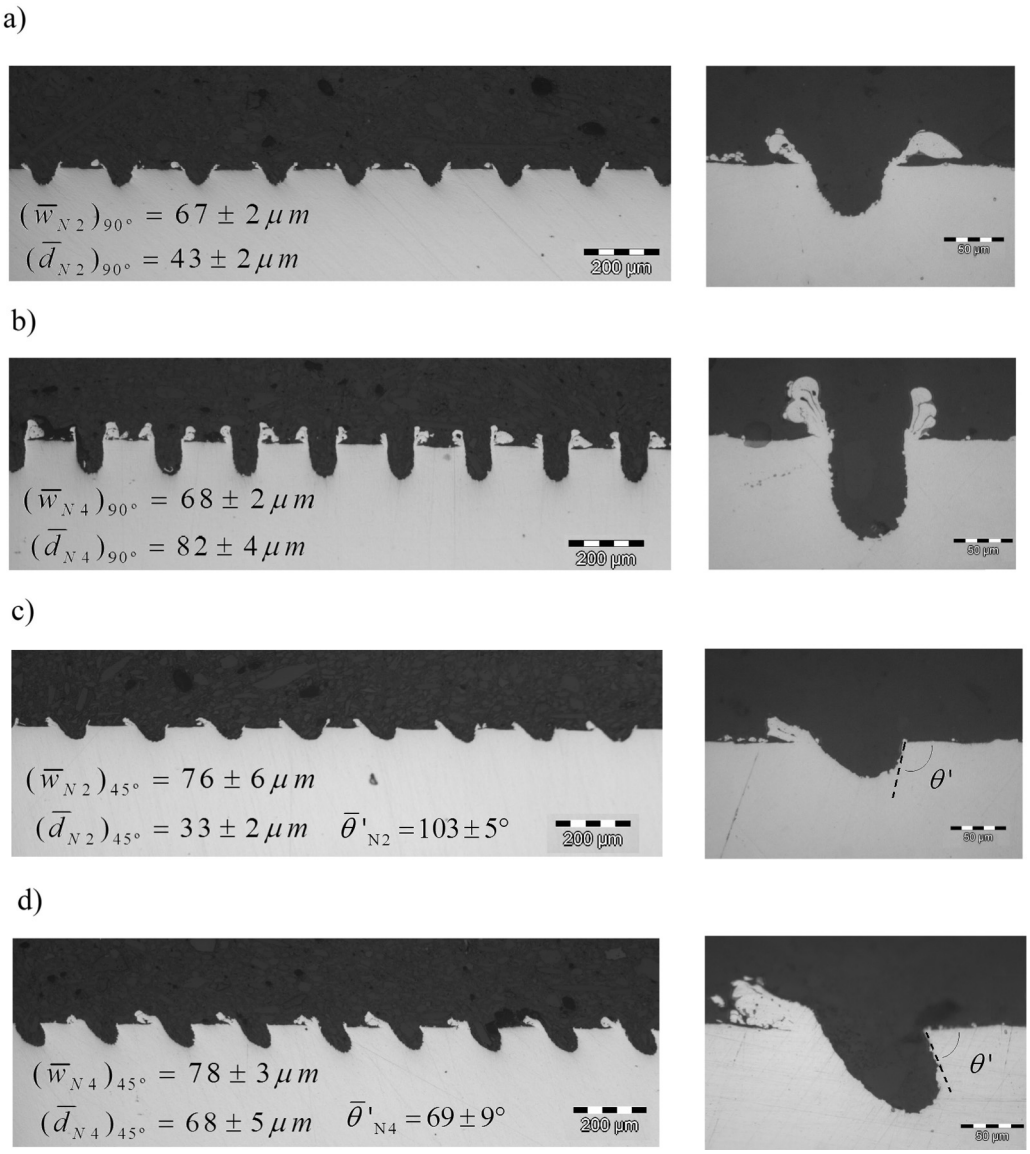

Fig. 4. Cross sections of microstructures on HC420LA by nanosecond pulses for (a) $N_{tracks} = 2$, $\theta = 90°$ (MC = 2); (b) $N_{tracks} = 4$, $\theta = 90°$ (MC = 4); (c) $N_{tracks} = 2$, $\theta = 45°$ (MC = 10); (d) $N_{tracks} = 4$, $\theta = 45°$ (MC = 12).

tion of the laser beam and the metal surface (Fig. 3b). An alignment angle value of 45° was considered with the aim of generating an additional mechanical interlock between polymer and metal (Schricker et al., 2014). As it will be shown later, the real alignment angle of the groove respect to the metal surface is not always equal to the planned alignment angle due to the dependence on the groove depth, which is directly related to the number of iterations (N_{tracks}). Therefore, the concept of internal cavity angle θ' (Fig. 3b) is introduced as an estimation of the real angle of the tilted groove: angle between the original surface of the metal and the wall of the groove. On the other hand, the influence of groove orientation is considered in order to analyze the possible differences between longitudinal and transversal orientations with the small joining areas tested.

Table 1 gathers the different microstructure conditions whose effects on the mechanical performance were analyzed for two different joining areas. On a first step, the geometry of each individual groove was studied as a function of different microstructure parameters. Only the N_{tracks} and θ affect the shape of the grooves, while the $d_{c\text{-}c}$ and their orientation (transversal or longitudinal) play no role. Fig. 4 discloses the cross sections of the microstructures attained for the two levels of N_{tracks} and θ. Fig. 4a and b show the groove geometry for $N_{tracks} = 2$ and $N_{tracks} = 4$ respectively when $\theta = 90°$ is considered. The N_{tracks} has a remarkable effect on the groove depth and the amount of the recast material, producing deeper grooves with higher crests of recast material when increasing its value. The average groove width for $\theta = 45°$ exhibits a raise of around 13% compared to the case of $\theta = 90°$. The latter is due to the increase of the laser spot size as consequence of its projection. For microstructures generated at $\theta = 45°$ (Fig. 4c and d) twice deeper grooves were produced when the N_{tracks} was doubled. Besides, the groove depth for each value was slightly smaller than in the case of $\theta = 90°$. This can be explained by the fact that the laser spot on the focal plane is projected at 45°, increasing its area and hence decreasing the power density with respect to the normal incidence ($\theta = 90°$). The internal cavity angles were $103 \pm 5°$ and $69 \pm 9°$ for $N_{tracks} = 2$ and $N_{tracks} = 4$ respectively. The latter proves that, for a given alignment angle, the internal cavity angle depends on the number of iterations. The behavior of the recast material deposition was different depending on the alignment angle. In the case of $\theta = 90°$ the recast material grew symmetrically with respect to the groove center, whereas in the case of $\theta = 45°$ this effect took places at only one

of the groove edges. The recast material distribution in the case of $\theta = 45^\circ$ could be explained by two main reasons. Firstly, the configuration is not symmetric and thus, the ejected material from the groove was closer to the laser beam at one of the edges. Secondly, one of the groove walls was deeper than the other one. The latter involves a larger amount of ejected material and thus a larger amount of recast material. The topographical characterization of the microstructures shows that the standard deviation associated with the groove depth was less than the 7%. Thus, a high level of accuracy and control of the groove geometry can be accomplished by the nanosecond pulses on HC420LA steel.

4. Results and discussion

4.1. Mechanical performance of T-joints

After metal pre-treatment, the specimens were joined and mechanically tested. Fig. 5a and b disclose the joint strength for different microstructure conditions (Table 1) considering 2.5 mm and 4 mm polyamide thickness respectively. The joint strength seems to be unaffected by the joining area, judging from the analogous trends observed for both areas. The mechanical results for both polyamide thicknesses suggest:

- A meaningful influence of distance between groove centers ($d_{c\text{-}c}$) on the mechanical performance of T-joints. When $d_{c\text{-}c} = 200\ \mu m$ is considered the joint strength is 3.4 times higher than in the case of $d_{c\text{-}c} = 600\ \mu m$. It could be explained based on the increase of the structure density by a factor of three when the distance between groove centers is reduced from 600 μm to 200 μm.
- An increase of the joint strength of about 27% is revealed in the case of deeper grooves ($N_{tracks} = 4$, MC = 3, 4, 7, 8, 11, 12, 15, 16) compared to shallower ones ($N_{tracks} = 2$, MC = 1, 2, 5, 6, 9, 10, 13, 14) keeping the remaining microstructure parameters constant.
- There is no evidence of influence of structuring orientation on the T-joints mechanical performance.
- The effect of alignment angle (θ) for a given set of microstructure parameters seems to be negligible. For both polyamide thicknesses, the dark bars ($\theta = 90^\circ$) show similar joint strength values to those of the corresponding light bars ($\theta = 45^\circ$) when the standard deviations are considered. The fact that the internal cavity angles are higher than 60° involves that, even if the grooves are completely filled by the melted polymer, there is no presence of metal material directly above the bottom of the groove, which could add an additional mechanical resistance. Also two of the geometrical features of the microstructures generated at $\theta = 45^\circ$ could cancel out the expected improvement of the mechanical interlock. The first factor is associated to the lower height and the different distribution of the recast material (at only one of the groove edges). Secondly, the fact that the groove width increases around 13% as compared to the microstructure produce at $\theta = 90^\circ$ could also contribute negatively to the mechanical interlock (Engelman et al., 2015; Schricker et al., 2014).
- The results reveal an important standard deviation associated to the average joint strength values. A previous study (Rodríguez-Vidal et al., 2014), which considers analogous microstructure patterns as pre-treatment, shows low deviation levels. Hence, the high standard deviation values could be associated to the small joining area and/or the joining configuration as well as the specimen preparation process.

The results analyzed above disclosed that, for the considered range of microstructure parameter values, an effect on the T-joints mechanical performance was only evidenced for the number of iterations (N_{tracks}) and distance between groove centers ($d_{c\text{-}c}$). An average increase of joint strength of around 200% was observed when the structure density was increased by a factor of three, while the average increase when doubling the number of iterations (depth) was of about a 27%. The results suggest that the superficial modification of the metal (structure density) has a more remarkable effect on the mechanical behavior than the volume modification (groove depth).

The effect of geometric parameters for microscopic structures was previously studied, by different authors, considering lap-joint configuration. Roesner et al. (2011) revealed the structure density as a key parameter to increase the steel–polyamide joint strength conducted by induction technique. Similar results were observed by Amend et al. (2014) in the case of aluminum–polyamide laser joints. They extended the study to the influence of the material thickness of the joining parts on the joint connection. Schricker et al. (2014) found out the structure depth and structure density as significant parameters for aluminum–polyamide assemblies. In this case the micro-structuring process was performed by a milling operation. Moreover, they analyzed the effect of the alignment angle of the structures (grooves and holes) on the joint shear strength. The study suggested a direct correlation of joint shear strength to the microstructures independent from alignment angle.

Based on the finding concerning the dependence of the internal cavity angle on the number of iterations, an additional microstructure condition was analyzed with the aim of matching the alignment (θ) and internal cavity angles (θ'). Thus, an additional mechanical interlock effect could be assumed due to the presence of metallic material directly above the bottom of the groove. Fig. 6 discloses the groove geometry when the microstructures are produced at $\theta = 45^\circ$ and $N_{tracks} = 6$. Consequently, the θ' was reduced down to $45 \pm 4^\circ$. The average groove width was reduced around 24% with respect to the structures produced at $N_{tracks} = 4$ due to the larger amount of ejected material being placed on the top of the groove wall (Engelmann et al., 2015). Furthermore, the recast material grows at the two edges of the groove as a consequence of the increase of molten material ejected from the cavity by the vapour and plasma pressure.

The microstructure detailed in Fig. 6 was generated in five specimens, keeping constant the remaining parameters with respect to MC = 12. After the joining process the T-joints were mechanically tested and the joint strength values (Fig. 7) did not evidence an influence of the internal cavity angle on the T-joints mechanical performance. Further inspections about the failure mode and the filling degree of the cavities are presented in the next section in order to better understand the mechanical results.

4.2. Examination of the fracture areas

A comprehensive inspection of the detached surfaces (joining interfaces of both metallic and polymer parts) was carried out for the different microstructure conditions. Since the microstructuring parameters which affect the groove geometry are the number of tracks and the alignment angle, the microstructure conditions selected for this analysis were: MC = 2 ($N_{tracks} = 2$, $\theta = 90^\circ$), MC = 4 ($N_{tracks} = 4$, $\theta = 90^\circ$), MC = 10 ($N_{tracks} = 2$, $\theta = 45^\circ$) and MC = 12 ($N_{tracks} = 4$, $\theta = 45^\circ$). In all cases the distance between groove centers was $d_{c\text{-}c} = 200\ \mu m$ and a transversal orientation of the grooves was considered.

Fig. 8a and b showS the top view SEM images of metal and polyamide parts respectively for MC = 4 as well as the corresponding detailed views of a representative groove. In the case of the metal part (Fig. 8a), the extended top view reveal that there are no traces of polyamide material hooked into the grooves. The detailed top view shows the groove (1, darkest area), the recast material (2, the lightest area) as well as the unprocessed metal between the recast material (3). The polyamide surface (Fig. 8b) discloses

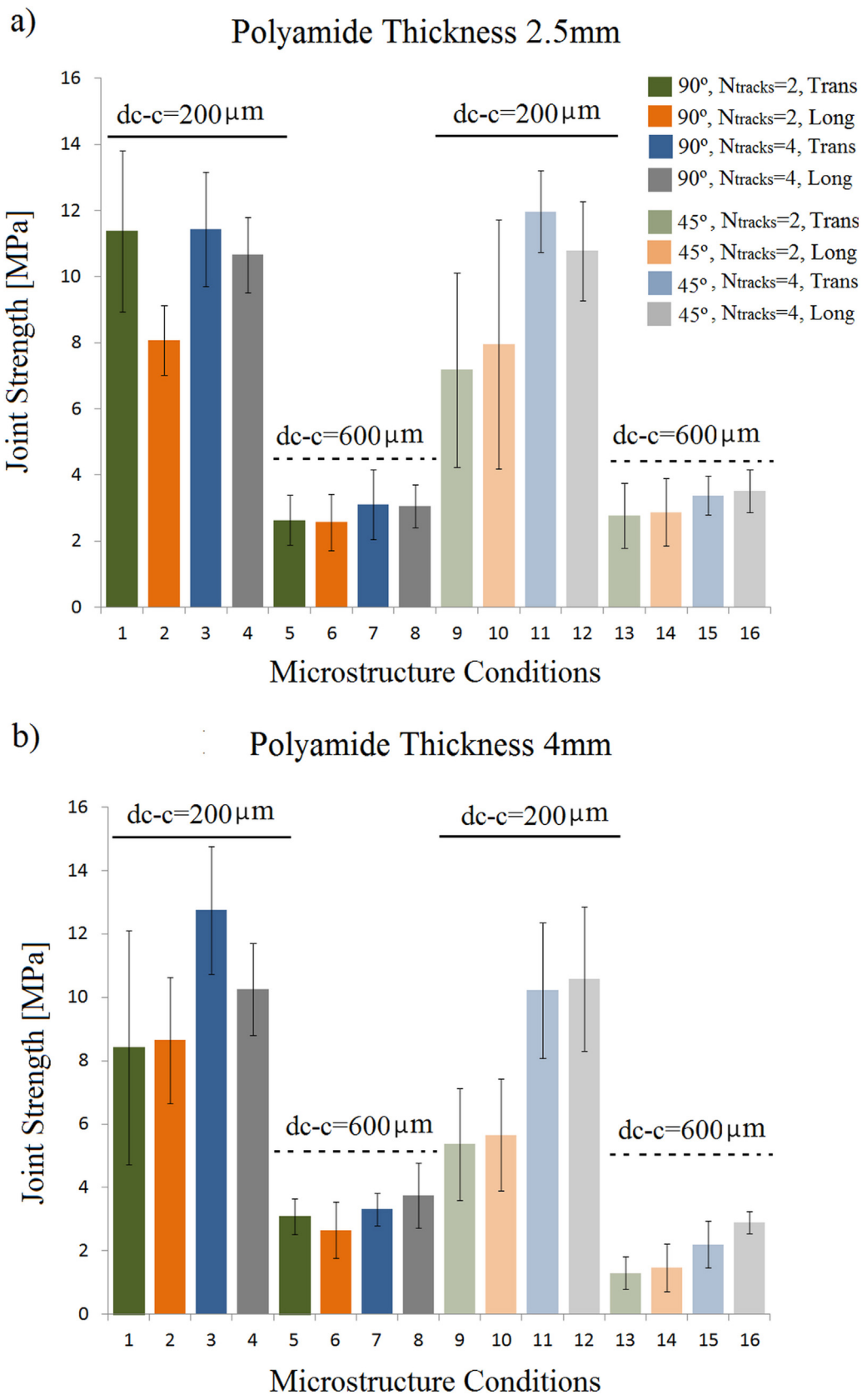

Fig. 5. Joint strength obtained from pull tests for HC420LA + PA6-GF30 for the different microstructure conditions in the case of (a) 2.5 mm polyamide thickness; (b) 4 mm polyamide thickness.

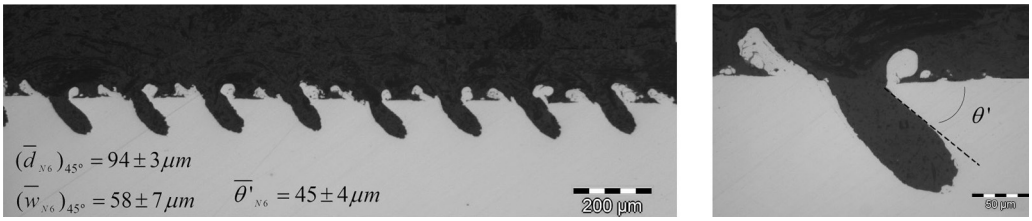

Fig. 6. Cross section of microstructures on HC420LA by nanosecond pulses for N_{tracks} = 6 and θ = 45°.

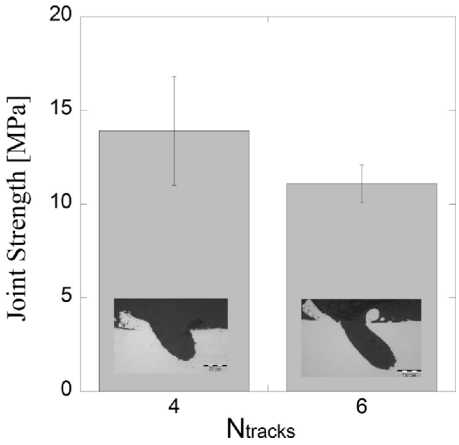

Fig. 7. HC420LA + PA6-GF30 joint strength achieved from pull-out tests for N_{tracks} = 4 and N_{tracks} = 6, keeping constant the remaining parameters: θ = 45°, d_{c-c} = 200 µm, transversal lines and 4 mm polyamide thickness.

a highly regular imprinted pattern that corresponds to the negative of the microstructure produced on the metal part. Thus, a clear ridge (1′, the lightest zone) can be associated to the replication of the groove as well as the irregular grooves produced by the recast material of the metal (2′, the darkest zone). The material between the irregular grooves (3′) corresponds to the unprocessed area of the metal (3).

The morphological features of the three remaining microstructure conditions (MC = 2, 10, 12) provided similar trends concerning the generation of regular imprinting patterns on the polymer parts. This fact reveals that in all cases the melted polymer was introduced into the metal grooves during the laser joining, although the quantity remained unknown at this stage.

On a second step, a topographical characterization of the polyamide surfaces was conducted to quantify the grooves filling degree during the joining process. Fig. 9a discloses the detailed SEM top views of the polyamide parts corresponding to the joining with microstructures conditions MC = 2 and MC = 4. Fig. 9b shows a comparison between 2000 µm long profiles measured on the polyamide surfaces disclosed in Fig. 9a in the transversal direction with respect to the imprinted ridges. Highly regular imprinted patterns were found for both MC, where the average ridge heights (1′) for MC′ = 2 and MC′ = 4 patterns were of 39 µm and 78 µm respectively. Based on the depth values measured on the microstructures produced on the metal parts for the MC = 2 (Fig. 4a) and MC = 4 (Fig. 4b), it is reasonable to assume that the melted polymer completely filled the microstructure volume of the grooves during the joining process.

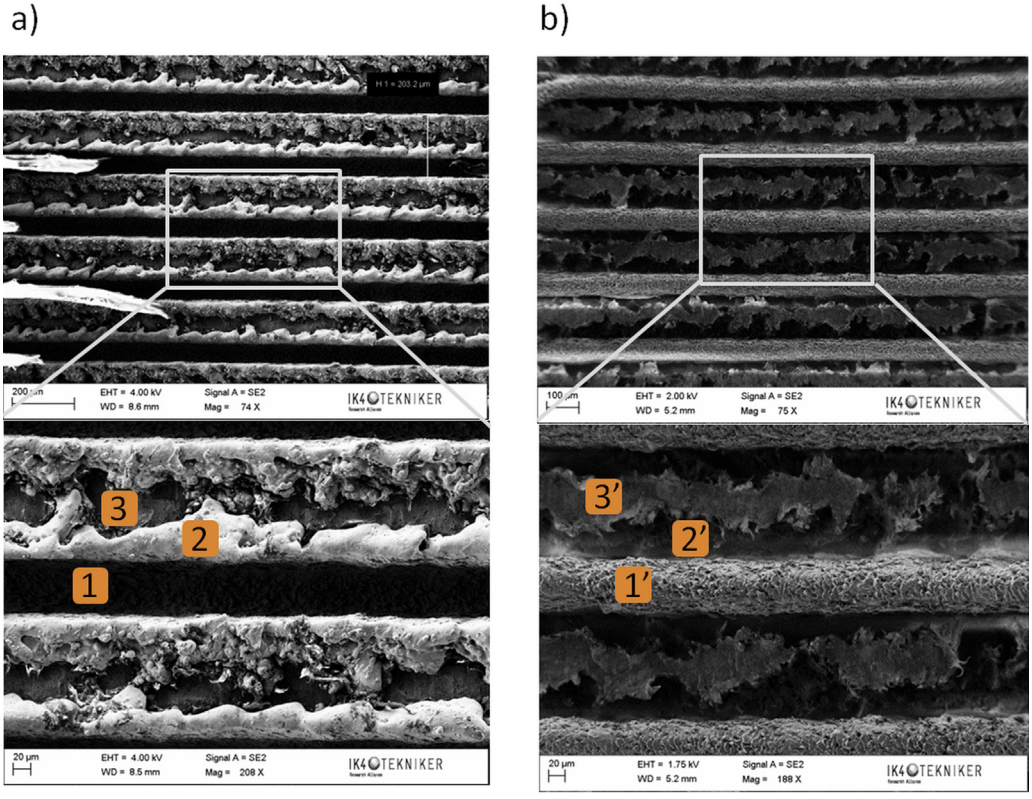

Fig. 8. Top view SEM images of (a) metal HC420LA; (b) polymer PA6-GF30 surfaces after pull-out tests for MC = 4 (Table 1): θ = 90°, N_{tracks} = 4.

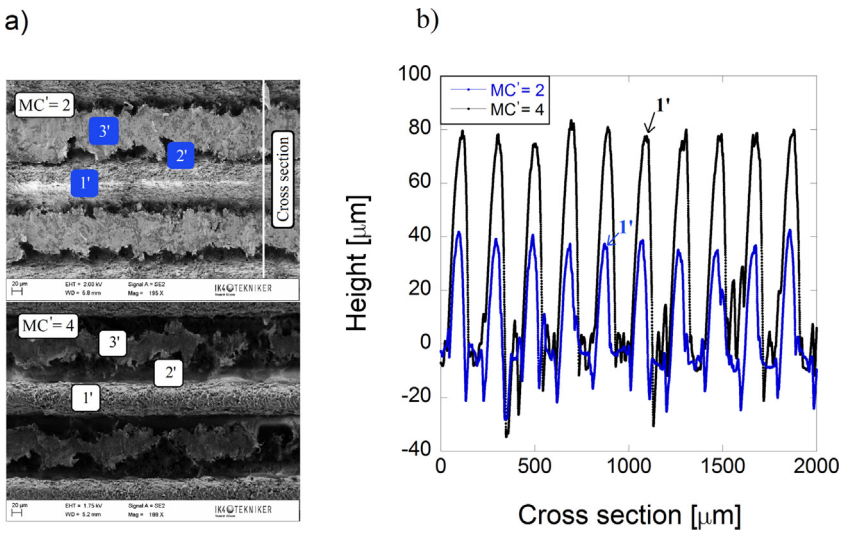

Fig. 9. (a) Top view SEM images of the polymer PA6-GF30 part after pull-out tests for the microstructure conditions MC = 2 (N_{tracks} = 2, θ = 90°) and MC = 4 (N_{tracks} = 4, θ = 90°); (b) transversal profiles of the polyamide imprinted patterns.

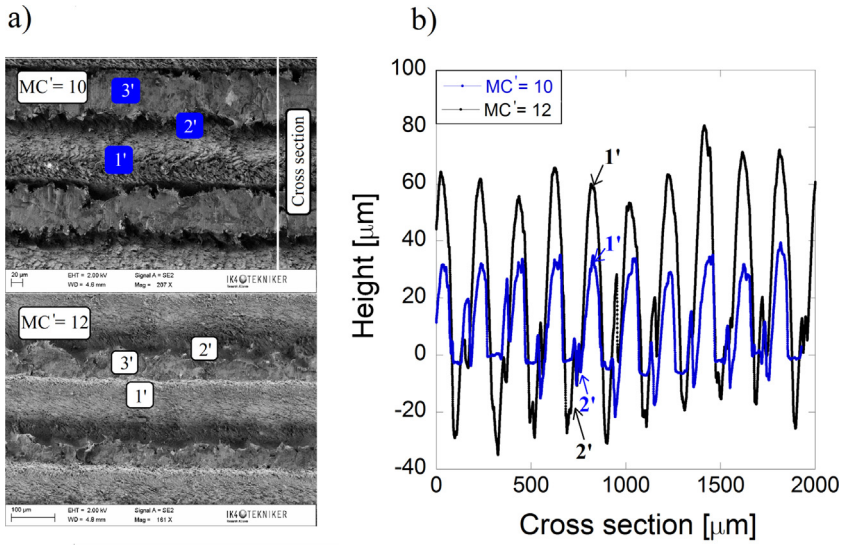

Fig. 10. (a) Top view SEM images of the polymer PA6-GF30 part after pull-out tests for the microstructure conditions MC = 10 (N_{tracks} = 2, θ = 45°) and MC = 12 (N_{tracks} = 4, θ = 45°); (b) transversal profiles of the polyamide imprinted patterns.

An analogous characterization (Fig. 10) was conducted for an alignment angle of 45°: MC = 10 and MC = 12. In the case of MC′ = 12 (Fig. 10a) the effect of the recast material (2′) was observed at only one groove edge, which evidences the tilt of the ridge. Although the profilometer is unable to provide a complete cross section in the case of tilted patterns, the peak height of the cross section can be considered as a reliable measurement. The average peak heights of the MC′ = 10 and MC′ = 12 imprinted patterns were of around 30 μm and 60 μm respectively. Once again, the average peak height values of the ridges are quite close to the groove depths of the corresponding microstructures generated on the metal part: MC = 10 (Fig. 4c) and MC = 12 (Fig. 4d).

Previous features allow concluding that the melted polymer completely filled the grooves due to the fact that the fill factors (defined as the ratio between the groove depth of the metal part and the peak height of the ridges imprinted on the corresponding polyamide part) found for the different MC, range from 88% to 95%. It ratifies the reliability of the mechanical trends shown in Fig. 5 and the interfacial failure between polymer and metal parts occurred for the grooves with different geometries.

Fig. 11a discloses the morphological characterization of the metal part (before joining), in the case of microstructures produced at $\theta = 45°$ and $N_{tracks} = 6$ $\left(\left(\theta'\right)_{N_{tracks}=6} = 50 \pm 4°\right)$, and Fig. 11b shows the corresponding part after the joining process and pull out tests. The comparison between them allows identifying the presence of polyamide traces hooked into the cavities (Fig. 11b, label 1). The latter involves an interfacial failure with polyamide breakage, which was ratified by the morphological feature of polyamide after pull out test (Fig. 11c). Six different measurements were carried out on the polyamide surface to guarantee reliable results due to the surface heterogeneity. Fig. 11d reveals that the peak height values of the non-hooked ridges (label 1′) are of around 90 μm. The latter suggests that the melted polyamide reaches the bottom part of the groove (Fig. 6). The different failure modes could be explained based on the fact that, as consequence of the decrease of the internal cavity angle, different load components are involved during pull out tests. Moreover, due to the decrease of groove width (Fig. 6), the polymer inserted inside the grooves becomes thinner and more fragile. Thus, the polyamide inserted into the grooves breaks at

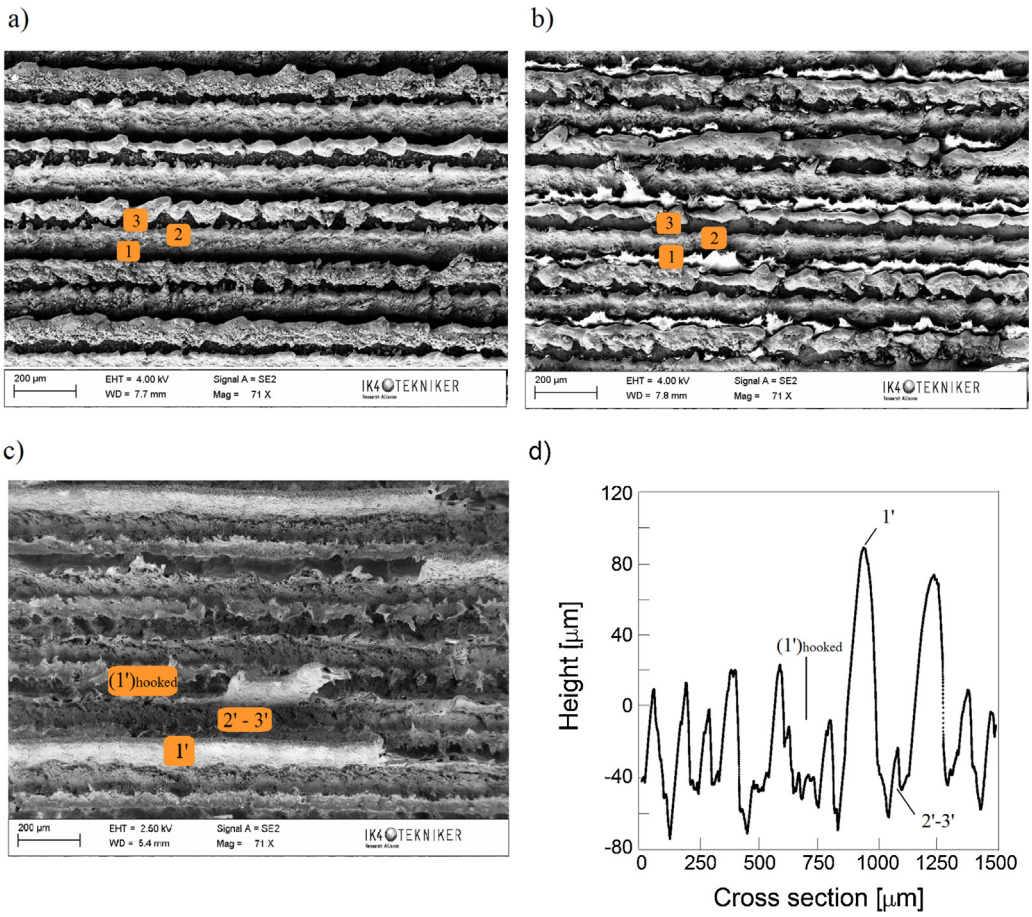

Fig. 11. Top view SEM images (a) microstructure patterns before joining; (b) metal and (c) polyamide after joining process and pull-out tests for the microstructure conditions $N_{tracks} = 6$, $\theta = 45^{\circ}$, $d_{c\text{-}c} = 200\ \mu m$; (d) transversal profile of the polyamide imprinted pattern.

strength values around those found in the case of an internal cavity angles at 90° (Fig. 7). Hence, there is no evidence of additional mechanical interlock with internal cavity angle of around 45°.

5. Conclusions

- The metal pretreatment by nanosecond pulsed laser depicts a precise and reliable method to ensure polymer-to-metal mechanical interlocking at the joint.
- The key microstructure parameter to improve the mechanical interlocking was the distance between adjacent grooves ($d_{c\text{-}c}$). A less significant influence on the T-joint mechanical performance was found for the number of iterations (N_{tracks}).
- The considered range of joining areas and the structuring orientation did not affect the joint strength values. Firstly, a dependence of internal cavity angle with number of iterations was evidenced. At higher number of iterations, the internal cavity angles approached 45°. Secondly, a different failure mode was found when the internal cavity angle was close to 45°. Nevertheless an additional joint strength improvement was not evidenced.
- The morphological and topographical features of the detached surfaces after pull-out tests showed that the volume of the different groove geometries (MC1-MC16) was completely filled during the laser conductive joining process.

Acknowledgements

The research leading to these results has received funding from the European Union's Seventh Framework Programme (FP7/2007-2013) under grant agreement 309993, PMJoin project. Authors thank the European Commission and the Consortium for the outstanding discussions that have led to elaborate this paper.

References

Amend, P., Mohr, C., Roth, S., 2014. Experimental investigations of thermal joining of polyamide aluminum hybrid using a combination of mono- and polychromatic radiation. Phys. Procedia 56, 824–834, 8th International Conference on Laser Assisted Net Shape Engineering LANE2014.

Amend, P., Pfindel, S., Schmidt, M., 2013. Thermal joining of thermoplastic metal hybrids by means of mono- and polychromatic radiation. Phys. Procedia 41, 98–105.

Bergmann, J.P., Stambke, M., 2012. Potential of laser-manufactured polymer–metal hybrid joints. Phys. Procedia 39, 84–91.

Cenigaonaindia, A., Liebana, F., Lamikiz, A., Echegoyen, Z., 2012. Novel strategies for laser joining of polyamide and AISI 304. Phys. Procedia 39, 92–99.

Engelmann, C., Meier, D., Olowinsky, A., Kielwasse, M., 2015. Metal meets composite-hybrid joining for automotive applications. LIM 2015-Lasers in Manufacturing.

Grujicic, M., Sellapan, V., Omar, M.A., Seyr, N., Obieglo, A., Erdmann, M., Holzleitner, J., 2008. An overview of the polymer-to-metal direct-adhesion hybrid technologies for load-bearing automotive components. J. Mater. Process. Technol. 197, 363–373.

Heckert, A., Zaeh, F., 2014. Laser surface pre-treatment of aluminium for hybrid joints with glass fibre reinforces thermoplastics. Phys. Procedia 56, 1171–1181, 8th International Conference on Laser Assisted Net Shape Engineering LANE2014.

Hussein, F., Akman, E., Oztoprak, B., Gunes, M., Gundogdu, O., Kacar, E., Hajim, K.I., Demir, A., 2013. Evaluation of PMMA joining to stainless steel 304 using pulsed Nd:YAG. Opt. Laser Technol. 49, 143–152.

Jung, K.W., Kawahito, Y., Takahashi, M., Katayama, S., 2013. Laser direct joining of carbon fiber reinforced plastic to zinc-coated steel. Mater. Des. 47, 179–188.

Kawahito, Y., Tange, A., Kubota, S., Katayama, S., 2006. Development of Direct Laser Joining for Metal and Plastic ICALEO, Paper #604.

Katayama, S., Kawahito, Y., Niwa, Y., Kubota, S., 2007. Laser assisted metal and plastic joining. Proceedings of the 5th Laser Assisted Net Shape Engineering, 41–51.
Roesner, A., Scheik, S., Olowinsky, A., Gillner, A., Poprawe, R., Schleser, M., Reisgen, U., 2011. Innovative approach of joining hybrid components. J. Laser Appl. 23, 1–6.
Rodríguez-Vidal, E., Lambarri, J., Soriano, C., Sanz, C., Verhaeghe, G., 2014. A combined experimental an numerical approach to the laser joining of hybrid polymer–metal parts. Phys. Procedia 56, 835–844, 8th International Conference on Laser Assisted Net Shape Engineering LANE2014.
Schricker, K., Stambke, M., Bergmann, J.P., Bräutigam, K., Hecncjell, P., 2014. Macroscopic surface structures for polymer-metal hybrid joints manufactured by laser based thermal joining. Phys. Procedia 12, 782–790, 8th International Conference on Laser Assisted Net Shape Engineering LANE2014.